Colloid Polym Sci 274:525–531 (1996)

ORIGINAL CONTRIBUTION

J.F. Widmann
E.J. Davis

Photochemical initiated polymerization of single microdroplets

Received: 2 September 1995
Accepted: 12 December 1995

J.F. Widmann · Prof. Dr. E.J. Davis (✉)
Department of Chemical Engineering
Box 351750
University of Washington
Seattle, Washington 98195-1750, USA

Abstract The production of polymeric microspheres via aerocolloidal processing is explored. A droplet consisting of a mixture of 1,6-hexanediol diacrylate and trimethylolpropane ethoxy triacrylate monomers was levitated electrodynamically in the path of an argon ion laser beam ($\lambda = 488$ nm). The laser beam served as the source of illumination for elastic and inelastic light-scattering measurements. The reaction was followed by Raman spectroscopy, and polymerization was initiated with an α-amino acetophenone derivative which undergoes α-cleavage upon exposure to the laser light. The diameters of the suspended droplets were typically 20–80 μm, producing polymeric microspheres of approximately the same size. The size and refractive index of the product microspheres were determined by elastic light-scattering. The Raman data show the elimination of carbon–carbon double bonds and the formation of C–H bonds as rapid polymerization proceeded.

Key words Aerocolloidal particles – light scattering – microspheres – Raman spectroscopy – photochemical polymerization

Introduction

The production of microspheres via the polymerization of aerosols has been investigated as an alternative to conventional emulsion-polymerization methods. The polymerization of aerocolloidal monomer droplets offers several advantages: i) the need for large volumes of liquid can be eliminated, ii) there are no interactions with the container walls, iii) ultra-pure colloids can be produced because surfactants are not required, and iv) the size of the microspheres can be controlled over a wide range.

Two approaches have been reported for the production of microparticles by aerocolloidal processing: i) the laminar flow aerosol reactor and ii) the vibrating orifice aerosol generator. It is also possible to use spray nozzles to generate fine droplets, but this leads to a highly polydisperse product. Matijević and his coworkers [1–3] used a laminar flow tubular reactor to produce polymeric microparticles. A monodisperse monomer aerosol was first generated by condensing vapor on condensation nuclei flowing through a temperature-controlled tube. The laminar flow stream was then contacted with a gas phase initiator to promote polymerization. Nakamura et al. [1] produced polymer and copolymer colloids with modal diameters up to 30 μm in this manner using trifluoromethanesulfonic acid (TSFA) as the gas phase initiator. Partch and his coworkers produced poly-*p*-tertiarybutylstyrene microspheres [2] and mixed polyureametal oxide particles [3]. Matijević [4] reviewed the subject of chemical reactions with aerosols. A disadvantage of the laminar flow reactor is that the residence time of aerosols in the reactor is a function of radial position, and this can lead to polydispersity [5].

Recently, Esen and Schweiger [6] demonstrated that polymeric microspheres of very uniform size can be

Colloid & Polymer Science, Vol. 274, No. 6 (1996)

produced by using a vibrating orifice generator to pass a stream of monomer droplets through a column illuminated by UV sources to photochemically initiate polymerization. They used a mixture of acrylate monomers (SOMOS 3100 from DuPont) to make polymer spheres with diameters of 5 to 50 μm.

The design and optimization of such aerosol polymerization processes require information on the polymerization rate, and this led Ward et al. [7] to explore the rates associated with monomer droplet polymerization using a single droplet technique based on levitation of a small droplet in an electrodynamic balance (EDB). They followed the polymerization process by adding a small amount of the fluorophore auramine-O to a droplet of acrylamide. Auramine-O does not fluoresce in low-viscosity media, but exhibits strong fluorescence as the viscosity is increased [8]. Thus, they were able to follow photochemically initiated polymerization by detecting and recording the increasing fluorescence as polymerization proceeded. Ward and his coworkers reported reaction times on the order of dozens of seconds for their system, with complete polymerization occurring within 1 min for microdroplets of order 10 μm in diameter.

It was the objective of this research to investigate more rapid polymerizations using the single particle method introduced by Ward et al. using Raman spectroscopy rather than fluorescence methods to follow the reaction.

The photochemically induced polymerization of acrylic monomers has been extensively studied and has proved to be an excellent method of applying durable surface coatings with low levels of volatile organic compounds [9]. These systems have been found to cure within fractions of a second upon irradiation with UV light [10]. A variety of methods has been developed for studying the polymerization of UV curable coatings, the most versatile of which is real-time infrared spectroscopy. Decker and Moussa [11] detected changes as small as 1% in the monomer concentration for a 1-μm-thick coating. They were also able to follow the kinetics of reactions occurring on the order of milliseconds. Unfortunately, this technique is inadequate for studying the polymerization of microdroplets, since it requires the sample to be applied to a KBr window.

In this research, a double-ring electrodynamic balance coupled to a Raman spectrometer was used to study the formation of a copolymer aerosol.

Experimental aspects

Materials

The two monomers used were 1,6-hexanediol diacrylate (HDDA) and trimethylolpropane ethoxy triacrylate (TMPEOTA). The HDDA was obtained from Henkel Corp. and the TMPEOTA from UCB Radcure Inc. Both monomers were used as received without further purification. The photoinitiator was Irgacure 369 from Ciba–Geigy Corp.

Trimethylolpropane ethoxy triacrylate is a tri-functional monomer with a viscosity of 60 cps at 25 °C. HDDA is a di-functional reactive diluent with a viscosity of 6 cps at 25 °C. These monomers were chosen to provide a balance between low viscosity and high reactivity. Irgacure 369 is a cleavage type photoinitiator capable of producing free radicals to initiate polymerization.

Equipment and methods

The experimental apparatus, shown in Fig. 1, has been described in detail previously [12, 13], so we need only to briefly summarize its features here. An electrodynamic balance (EDB) was coupled to a Raman spectrometer and light-scattering detectors. The EDB was used to suspend a charged liquid aerosol by means of superimposed AC and DC electric fields. The DC field was used to balance the vertical forces on the particle such as gravity, drag and the photophoretic force from the laser beam. The particle was stabilized in the center of the chamber by the AC field. The levitated droplet was illuminated from below by a vertically polarized argon ion laser operating at a wavelength of 488 nm. The laser provided the illumination for elastic and inelastic (Raman and fluorescence) light-scattering measurements. By detecting the light scattered elastically by the particle with a 512 pixel photodiode array and a photomultiplier tube (PMT) which measured the light scattered at right angles to the laser beam, information

Fig. 1 The experimental apparatus used for the study

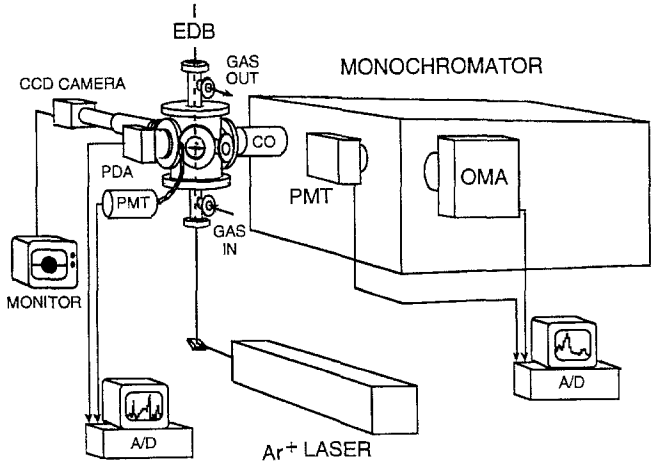

about the refractive index and size of the droplet was obtained by comparing the scattered intensities with Mie theory [14]. The inelasticity scattered light (Raman scattering) was used to probe the Raman-active molecular bonds of the sample. The apparatus was also plumbed so that oxygen and nitrogen could be introduced into the chamber.

To determine the droplet size, the intensity of scattered light was measured as a function of the polar angle, θ, where θ is measured from the direction of propagation of the incident light beam. In these experiments, light was collected with the photodiode array over the range of polar angles $76.3° \leq \theta \leq 104.9°$. Scattered light was also collected with the PMT by means of an optical fiber mounted at $\theta = 90°$ and $\phi = 18°$, where ϕ is the azimuthal angle. The intensity of the light collected at one position (θ, ϕ) is an extremely sensitive function of the size and refractive index of the microsphere. If either the size or refractive index vary with time, large variations in the intensity occur, for the microsphere acts as a resonance cavity. At numerous combinations of size and refractive index constructive interference of the refracted and reflected light within the microsphere produce resonances [15]. The far-field intensity, which varies with time when the size and/or refractive index change, is called a resonance spectrum. By comparing the resonance spectrum with theory, the size and evaporation rate of a liquid droplet can be determined to about one part in 10^5 [16].

The angular scattering, measured with the photodiode array, is also sensitive to the size and refractive index. A graph of the scattered intensity versus angle is called a phase function. An estimate of the size can be obtained by simply measuring the number of peaks per polar angle and comparing that peak frequency with Mie theory. The peak frequency is relatively insensitive to the refractive index, but the fine structure of the phase function depends on both the size and refractive index.

To trap a droplet in the EDB, a small amount of liquid was placed at the end of a hypodermic needle and exposed to a short DC pulse of 4–5 kV. For low-viscosity fluids the electric pulse usually causes the liquid to explode into a polydisperse mist of small, charged particles. One of these particles is then trapped within the electric fields. For the monomers used in this study, the higher viscosity prevented the formation of a spray, and a single droplet was discharged from the needle. The formation of a single droplet permitted relatively large particles to be generated and trapped. In this experiment, monomer droplets in excess of 80 μm in diameter were suspended. The size of the final polymeric microsphere could be controlled by permitting the droplet to evaporate prior to polymerization. It is also possible to use a monomer mixture containing a volatile solvent to produce smaller microspheres by letting the solvent evaporate prior to polymerization.

Results and discussion

The evaporation rates of the individual monomers and the mixture were determined using the light-scattering measurements described above. Figure 2 shows a representative phase function for a TMPEOTA monomer droplet. Over the range of light-scattering size parameters, x ($x = 2\pi a/\lambda$), and refractive indices, n, encountered here, the peak frequency, $dP/d\theta$ (number of peaks per degree), varies linearly with x. Here λ is the wavelength of the incident light and a is the radius of the particle. An approximate relation between peak frequency and x for $100 < x < 500$ is given by

$$\frac{dP}{d\theta} = 0.0047\,x\,. \tag{1}$$

This approximation can be used to estimate the size of the particle to within a few percent. A more accurate determination of the size can then be carried out by comparing the measured phase functions with Mie theory. Also shown in Fig. 2 is the phase function computed from Mie theory for the TMPEOTA droplet (for $x = 242.4$ and $n = 1.4688$). For $x = 242.4$, the droplet radius is 18.82 μm. A change of ± 0.05 μm from the "best fit" changes the calculated phase function significantly so that the agreement between theory and experiment is poorer.

Resonance spectra clearly show the effects of evaporation on elastic light scattering. Figures 3 and 4 present resonance spectra for evaporating droplets of the individual monomers TMPEOTA and HDDA, respectively. Figure 3 suggests that the TMPEOTA was impure, for the evaporation rate, which is indicated by the resonance

Fig. 2 A comparison of experimental and theoretical phase functions for a droplet of TMPEOTA ($n = 1.4688$, $a = 18.82$ μm)

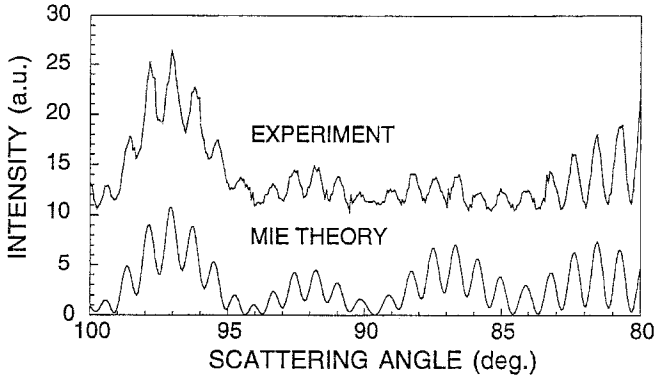

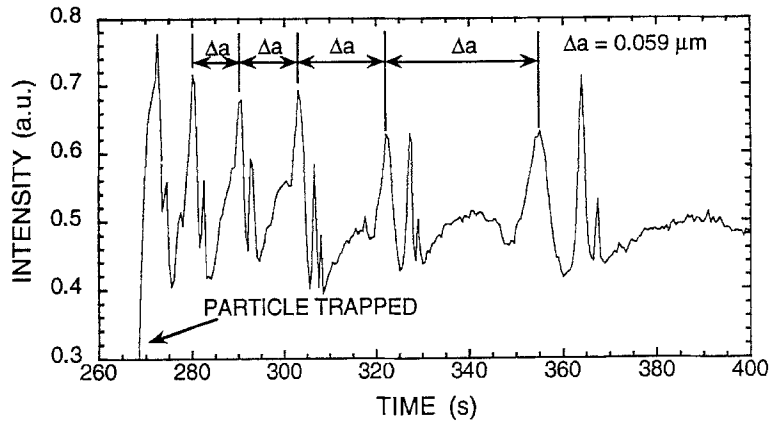

Fig. 3 An experimental reasonance spectrum for an evaporating droplet of TMPEOTA. The change in radius, Δa, between resonances is shown

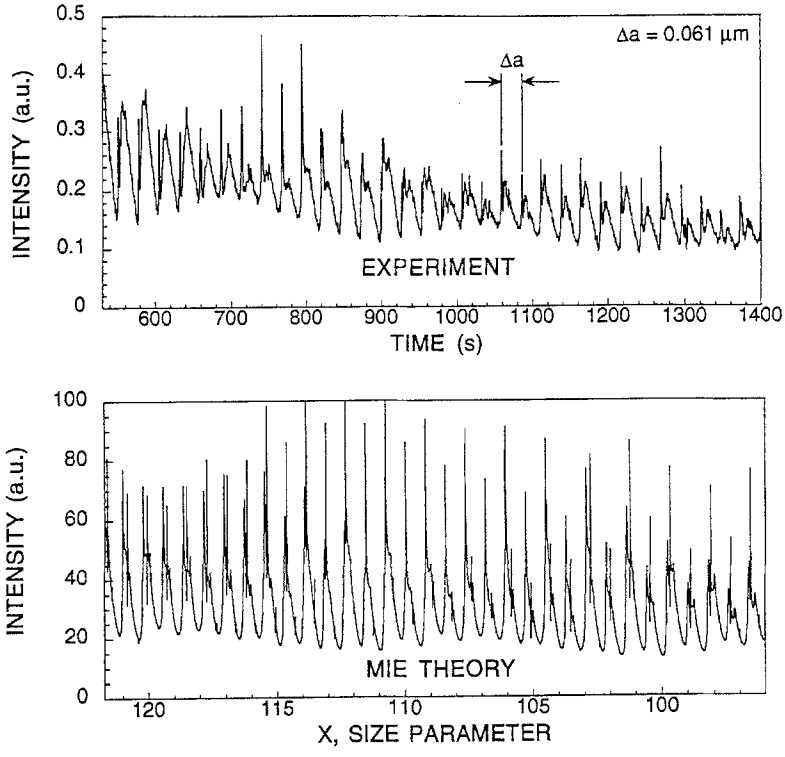

Fig. 4 A comparison between measured and calculated resonance spectra for an evaporating droplet of HDDA. The change in radius, Δa, between resonances is indicated

spacing, decreased with time as a more volatile component distilled from the sample. Based on Mie theory calculations, the major resonance peaks indicated in the figure have a spacing corresponding to $\Delta a = 0.059\ \mu m$. Even after an hour, the evaporation rate continued to decrease. In contrast, Fig. 4 indicates that the HDDA evaporated at a constant rate, suggesting a pure component. In this case the resonance spacing corresponds to a radius change of $0.062\ \mu m$. The evaporation rate, da/dt, was $-0.139\ \mu m/min$ for the times shown in the figure. The resonance spectrum obtained from Mie theory is also presented in the lower figure. The sharpest peaks appearing in the theoretical results do not appear in the experimental spectrum because the PMT output was processed and filtered such that the cutoff frequency removed them.

In addition to the elastically scattered light, the inelasticity scattered light was also collected. The Raman scattering was collected with a lens system and focused on the slit of a double monochromator (SPEX model 1403). The monochromator was equipped with two detectors, a single-channel photomultiplier tube with photon-counting electronics and a 600-channel optical multichannel analyzer. Schweiger [17] has reviewed recent work on microparticle Raman spectroscopy.

Raman spectra obtained for each of the individual monomers were indistinguishable. The Raman spectrum for a droplet containing a mixture of HDDA and TMPEOTA is shown in Fig. 5. Of particular interest are the peaks near 1630 cm^{-1}, 3040 cm^{-1}, and 3100 cm^{-1} associated with the carbon-carbon double bond. Since the C=C bonds are broken during polymerization, the changes in these peaks can be used to characterize the polymerization.

Radical induced polymerizations are known to be inhibited by O_2 due the high reactivity of O_2 with radicals. Photochemically induced polymerization can be considered to occur via two reactions in series. In the first reaction, free-radicals are produced from the initiator. In the second, the polymerization is initiated as the free-radical reacts with the monomer. In the presence of O_2 the free-radical can participate in an oxidation reaction, preventing the initiation step from occurring, as indicated in the following diagram.

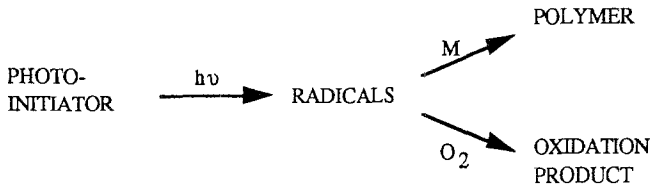

Decker and Jenkins investigated the O_2 inhibition of UV and laser-induced polymerizations of multi-acrylate systems [18]. They found that in a well-aerated system, the dissolved O_2 concentration was such that polymerization would not occur until the O_2 had been depleted via the production of radicals and the subsequent oxidation reaction. In the experiments described here, this posed a greater limitation for several reasons. In the polymerization of aerosols, the diffusion rate is fast compared to the planar coatings investigated by Decker and Jenkins because of the very small path length for diffusion in microdroplets. The high surface-to-volume ratio promotes rapid diffusion, maintaining high concentrations of O_2. Also, due to the spherical geometry, the electromagnetic field intensity is much greater near the surface of the droplet [19] than in its core. Thus, the rate of free-radical production is considerably less in the center of the droplet, where the lower concentration of O_2 would allow the polymerization to occur. Finally, the production of radicals is expected to be lower using visible light than with UV.

Two Raman spectra for a polymerized microsphere are presented in Fig. 6. The two scans correspond to the same particle, the upper one in the presence of N_2 only, the lower one with only O_2 present in the chamber. In the absence of oxygen, the polymer product exhibits strong fluorescence, which nearly masks the Raman signal. The fluorescence is substantially reduced as O_2 is introduced into the chamber, resulting in the lower spectrum. As indicated above, the presence of dissolved oxygen is known to reduce fluorescence and completely eliminate phosphorescence [20].

Investigation of the reaction kinetics is complicated by the fluorescence of the polymer product. The intensity of the fluorescence signal is much larger than the Raman intensity, making it difficult to follow the Raman signal during the reaction. Figure 7 shows the increase in Raman signal at 2940 cm^{-1}, which corresponds to the C–H bond, during a polymerization experiment. As expected, this peak grows during the polymerization as C–H bonds are formed. This peak can be detected despite the strong fluorescence. By flowing oxygen through the chamber the fluorescence could be suppressed, but it difficult to separate the effect of oxygen diffusion from the intrinsic

Fig. 5 A Raman spectrum of a liquid droplet consisting of equal mass fractions of TMPEOTA and HDDA

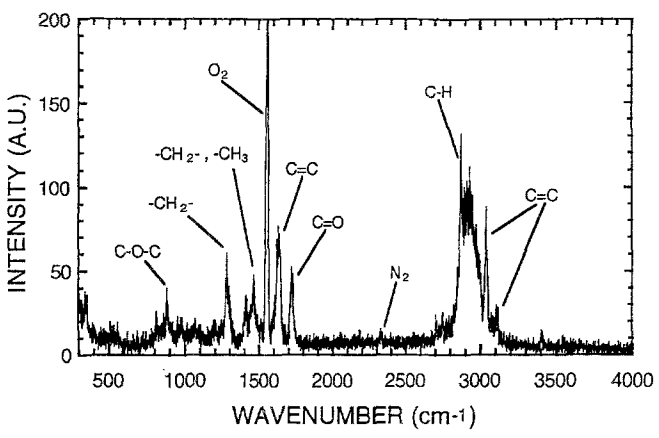

Fig. 6 Raman spectra for a polymer microparticle, showing the effect of oxygen

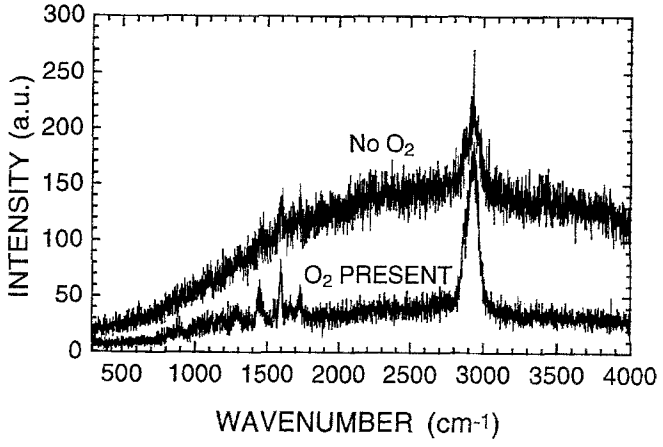

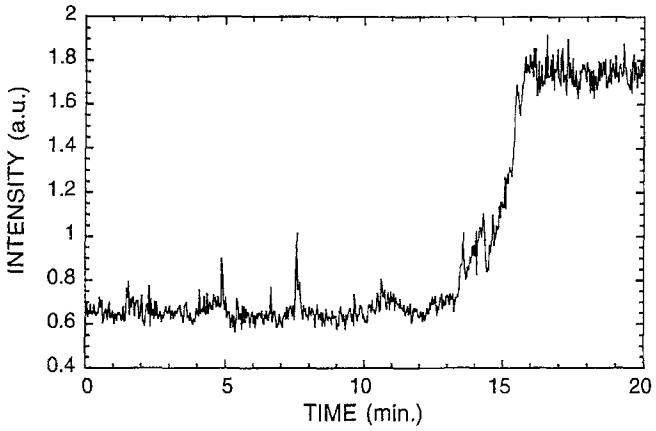

Fig. 7 The intensity of the Raman signal at 2940 cm^{-1} (the C–H bond) during polymerization in the presence of oxygen

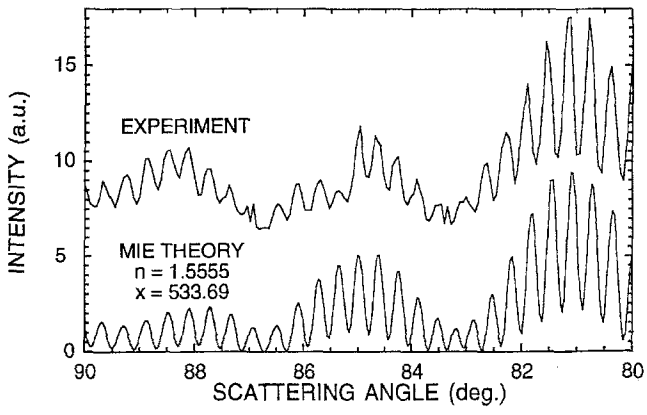

Fig. 8 Measured and calculated phase functions for a solid polymer microsphere with $a = 40.95$ μm and $n = 1.5555$

chemical kinetics. In this instance, the polymerization was observed to occur over the course of several minutes. This is because the reaction rate is limited by the rate of oxygen diffusion out of the particle. When a particle was trapped in an oxygen-free environment, the polymerization occurred within a few seconds or even faster. It was not possible to obtain spectra of the particles as they polymerized with the CW laser power available (approximately 1.0 W at $\lambda = 488$ nm). According to the absorption spectra provided by Ciba–Geigy Corp, Irgacure 396 should exhibit negligible absorption at wavelengths above 400 nm. Our results show that the absorption is sufficient at 488 nm to initiate polymerization.

The interpretation of the data was complicated by several factors. As discussed above, the presence of oxygen affects both the kinetics of the reaction and the fluorescence intensity. It is desirable to have oxygen present to quench the fluorescence so that a Raman spectrum may be obtained; however, the polymerization will not proceed if the dissolved oxygen consumes the radicals necessary to initiate polymerization.

The flow characteristics of the apparatus pose an additional complication. The EDB reactor behaves like a well-mixed chamber with a volume of 350 cm^3 and 11 cm^3 of inlet tubing [21]. This poses a problem when making a step change in the inlet gas composition during an experiment. Following a change in the inlet conditions, it takes several "space times" for the gas within the chamber to reach the inlet composition. The space time, τ_{EDB}, is defined as the volume of the reactor divided by the volumetric flow rate. For gas flow rates in excess of 80 cm^3/min, the particle stability is compromised, representing a lower limit of τ_{EDB} of approximately 4 min. After a step change in the inlet oxygen concentration, the oxygen concentration within the chamber varies exponentially with time. This changing gas concentration further complicates the interpretation of rate data.

The optical characteristics of the final product was obtained by light scattering. Figure 8 presents a measured phase function for a polymeric microsphere and the "best fit" phase function computed using Mie theory. We should note that the experimental phase function is based on "raw" data, that is, the individual pixels have not been calibrated to determine their quantum efficiencies, and optical corrections associated with the light collection system have not been made. Nevertheless, the agreement between measured and computed phase function is good, particularly with respect to the angular positions of the peak and troughs. The comparison between theory and experiment permits us to conclude that the particle was a sphere with a diameter of 81.90 ± 0.05 μm, and the refractive index was found to be 1.5555 ± 0.0005. We note that a change of ± 0.05 μm in diameter or ± 0.0005 in refractive index changes the calculated phase function significantly. The initial microsphere was composed of equal mass fractions of TMPEOTA and HDDA.

The increase in refractive index associated with the polymerization also appears to occur in the formation of polystyrene latex (PSL) microspheres. For styrene the refractive index is 1.5468 at 293 K, and that of PSL microspheres has been reported to be in the range 1.57–1.621 [22].

Conclusions

The photochemically induced polymerization of an aerocolloidal mixture of monomers has been explored by means of elastic and inelastic light scattering. It was demonstrated that polymeric microspheres can be produced by

such a process. The feasibility of using Raman spectroscopy to study aerosol polymerizations was also demonstrated. In this case the reaction was too fast to permit Raman spectra to be obtained during the course of the reaction, but the spectra taken before and after polymerization characterize the materials. The use of a high-intensity pulsed laser rather than a CW laser would permit Raman spectra to be obtained much faster. This would make it possible to follow the reaction process in more detail. The combination of elastic and inelastic light scattering measurements makes it possible to determine the optical properties and to chemically characterize the polymeric product.

Acknowledgment The authors are grateful to the National Science Foundation for Grant Number CTS-9120334 which supported this research.

References

1. Nakamura K, Partch RE, Matijević E (1984) J Colloid Interface Sci 99:118
2. Partch RE, Matijević E, Hodgson AW, Aiken BE (1983) J Polymer Sci Polymer Chem Ed 21:961
3. Partch RE, Nakamura K, Wolfe KJ, Matijević E (1985) J Colloid Interface Sci 105:560
4. Matijević E (1982) Heterogeneous Atmos Chem Geophys Monograph Series 26:44
5. Davis EJ, Liao SC (1975) J Colloid Interface Sci 50:488
6. Esen C, Schweiger G (1995) J Colloid Interface Sci, in press
7. Ward TL, Zhang SH, Allen T, David EJ (1987) J Colloid Interface Sci 118:343
8. Oster G, Nishijima Y (1956) J Amer Chem Soc 78:1581
9. Hoyle CE, Kinstle JF (1990) Radiation Curing of Polymeric Materials, American Chemical Society, USA
10. Decker C (1992) in: "Radiation Curing: Science and Technology", edited by Pappas SP, Plenum Press, New York
11. Decker C, Moussa K (1989) Macromolecules 22:4455
12. Rassat SD, Allen TM, Davis EJ (1993) in "Laser Applications in Combustion and Combustion Diagnostics", Proc. SPIE 1862:182
13. Foss WR, Li W, Allen TM, Blair DS, Davis EJ (1993) Aerosol Sci Tech 18:187
14. Bohren CF, Huffman DR (1983) "Absorption and Scattering of Light by Small Particles", John Wiley & Sons, USA
15. Hill SC, Benner RE (1988) in: "Optical Effects Associated with Small Particles", World Scientific, Singapore
16. Ray AK, Souyri A, Davis EJ, Allen TM (1991) Appl Opt 30:3974
17. Schweiger G (1990) J Aerosol Sci 21:483
18. Decker C, Jenkins AD (1985) Macromolecules 18:1241
19. Foss WR, Davis EJ (1995) Chem Eng Comm, in press
20. Guilbault GG (1973) "Practical Fluorescence: Theory, Methods, and Techniques", Marcel Dekker, New York
21. Rassat SD (1994) "Raman Spectroscopic Investigation of Gas-Solid Reactions of Single Microparticles", PhD Dissertation University of Washington, Seattle, WA
22. Davis EJ, Ravindran P (1982) Aerosol Sci Tech 1:337